On the quantitation of light emission from cytochrome c in the low quantum yield limit

P. M. Champion and R. Lange

Citation: The Journal of Chemical Physics **73**, 5947 (1980); doi: 10.1063/1.440153
View online: http://dx.doi.org/10.1063/1.440153
View Table of Contents: http://scitation.aip.org/content/aip/journal/jcp/73/12?ver=pdfcov
Published by the AIP Publishing

On the quantitation of light emission from cytochrome c in the low quantum yield limit

P. M. Champion[a] and R. Lange

Institut de Biologie Physico-Chimique, Fondation Edmond de Rothschild, Service de Biospectroscopie, 75005 Paris, France
and Institut National de la Santé et de la Researche Médicale, U 128 B.P. 5051, 34033 Montpellier, France
(Received 27 March 1980; accepted 16 July 1980)

A method for the quantitation of light emission is presented which uses the Raman scattering cross section of water as a reference. The method is successfully applied to systems having a known quantum yield, thus providing an independent check of Raman cross-section measurements. A very weak incoherent emission from the ferrocytochrome c system is quantitated ($\Phi = 3.6\times10^{-6}$) and interpreted using a simple kinetic model which is consistent with the quantum mechanical treatment. The quantum yield measurements imply that the excited state (S_1) lifetime of the ferrocytochrome is on the order of 0.2 ps, while the lifetime of the ferricytochrome is deduced to be much shorter. The implications of these measurements concerning the magnitudes of the excited state (S_1, S_2) damping factors in ferrocytochrome c are also discussed.

I. INTRODUCTION

Water is the natural solvent for living systems and, as might be expected, its physical properties strongly influence the characteristics of solute biomolecules. One striking example of this effect can be found by consideration of the absorption spectrum of water over a wide range of electromagnetic frequencies.[1] A precipitous drop of nearly eight orders of magnitude in the absorption coefficient takes place as the visible frequencies are approached from either the infrared or the ultraviolet. It is probably for this reason that a variety of chromophores crucial to life (e.g., chlorophylls, hemes) have evolved with very intense absorption bands located in this visible "window."

Since visible radiation is often used as an experimental probe of such systems (absorption, fluorescence, and scattering spectroscopies), it is desirable to quantitate the properties of water in this region for use as a natural reference standard. One such property of water which appears to be particularly useful is the scattering intensity of the broad Raman band (O–H stretching vibrations) located at a Stokes shift ($\Delta\nu$) of ~3300 cm^{-1}. By using the intensity of this band as a standard it is possible to quantitate rather simply (as will be shown below) the absolute quantum yields of systems which are either very dilute ($\sim10^{-9}$ M) or have very low quantum yields ($\Phi\sim10^{-6}$).

The heme proteins provide one good example of low quantum yield systems. The simple fact that resonance Raman scattering is observed in these proteins, and is not swamped by fluorescence, already gives a good indication of the short excited state lifetimes and low quantum yields that must be associated with the heme group. A quantitation of the excited state lifetime is, of course, very important for determination of the damping factor needed in the calculation of resonance Raman excitation profiles.[2] The question of the scale of the excited state lifetime in heme systems, particularly the heme group of cytochrome c, has prompted the present study. Earlier stimulating work on this subject has been carried out by Friedman, Rousseau, and Adar[3–5] but no absolute quantum yields of the cytochrome c system have been reported.

We present here a relatively simple method for obtaining absolute quantum yield information by referencing to the Raman scattering cross section of water; the technique is demonstrated using as examples sodium fluorescein, flavin adenine dinucleotide (FAD), and the cytochrome c system. Finally, we develop a simple kinetic analysis which is shown to be consistent with the quantum mechanical treatment and simultaneously includes the three important contributions (resonance scattering, resonance fluorescence, and relaxed fluorescence) to the light emission in the low quantum yield limit.

II. EXPERIMENTAL TECHNIQUE

A. Apparatus and materials

The light emission spectra are collected by means of a standard laser Raman spectrometer using a cooled RCA 31034 phototube. The monochromator is scanned over a large wave number range (typically ~5000 cm^{-1}) by means of a stepping motor drive while the phototube output current is amplified and recorded. The polarization response of the gratings is eliminated by scrambling the polarization of the collected light prior to its entrance into the Coderg DH 800 monochromator. Detection is at 90° to the incident laser beam and the polarization of the incident light is perpendicular to the scattering plane. Reabsorption of emitted or scattered light is largely eliminated by the use of dilute solutions and small scattering path lengths (<1 mm). The samples are held in standard 1×1 cm fluorescence cuvettes and the solution is constantly stirred with a small magnetic stir bar in order to minimize photodecomposition and sample degradation. The sample cuvette position is rigidly fixed by a special mount so that, once the system optics are aligned, the cuvettes can be exchanged reproducibly without affecting the signal intensity. Laser powers are typically in the 20–100 mW range.

[a]Present address: Laboratory of Atomic and Solid State Physics, Cornell University, Ithaca, N.Y. 14853.

 0021-9606/80/245947-11$01.00

The total response of the monochromator/detection system is carefully accounted for and all integrated intensities are corrected using the response curve. Integration of the scattered or emitted light is accomplished by cutting out and weighing the appropriate areas under the chart recorder trace. Scan speeds of the monochromator are adjusted digitally by means of the stepping motor so that narrow Raman lines (e.g., from benzene or sulfate) can be broadened on the chart recorder output by a known factor. Typical scan times are on the order of 15 min/spectra.

Before taking spectra of any emitting sample, the spectrum of the buffer or solvent is always accumulated. The sample, from a concentrated stock solution, is then added in known quantity using micropipettes. Although this is a time consuming process, it is well worthwhile since it eliminates buffer/solvent contamination problems and also gives good base lines which are needed for an accurate calculation of the emission intensities.

The sodium fluorescein samples are obtained from Eastman Kodak and Kuhlman and are used without further purification. The FAD and cytochrome c samples are purchased from Sigma Chemical Co. and used as received. Reduction of the cytochrome is carried out using a few grains of sodium dithionite. Water samples are typically double distilled in quartz and deionized. All absorption measurements are made using an Amin-co DW-2 spectrophotometer. Optical densities are measured easily down to the 10^{-2} range on this instrument; samples with optical densities below this range are prepared by careful dilution of stock solutions.

B. Method

The absolute quantum yield measurements are based on a comparison of the chromophore emission intensity to the Raman scattering intensity of the O–H stretching band of water. This band is located at $\Delta\nu \cong 3300$ cm^{-1} and has a width of about 400 cm^{-1}.[6] The band is polarized with a depolarization ratio of 0.16. To our knowledge there is only one scattering cross-section measurement of this band in the literature. For right angle scattering at 488 nm excitation, Kondilenko *et al.*[7] have measured $d\sigma_w/d\Omega = 9\times10^{-30}$ cm^2 sterad^{-1} molecule^{-1} by referencing to the absolute cross section of the 992 cm^{-1} line of benzene.[8] Kondilenko's value rises to 9.7×10^{-30} cm^2 sterad^{-1} molecule^{-1} if the cross section of the benzene line is taken as the average between the results of Ref. 8 and those of Skinner and Nilsen,[9] who have measured the 992 cm^{-1} line cross section by another method. We have also measured $d\sigma_w/d\Omega$ using a technique similar to that of Ref. 7. However, instead of referencing the broad water band directly to the very narrow (2.5 cm^{-1} width) 992 cm^{-1} line, we use the relatively broad (~10 cm^{-1}) 3060 cm^{-1} band of benzene as an intermediate intensity standard. This is a useful technique because it allows the measurements to take place without the use of neutral density filters to attenuate the peak height of the 992 cm^{-1} line as was necessary in Ref. 7. When the index of refraction correction[9] and the concentration ratios are taken into account, we find the scattering cross section of water (parallel plus perpendicular scattering; 488 nm excitation) to be $d\sigma_w/d\Omega = (11.8\pm2)\times10^{-30}$ cm^2 sterad^{-1} molecule^{-1}, which is in reasonable agreement with Kondilenko's result. Here we have taken an average value for the cross section of the 992 cm^{-1} line of benzene calculated from Refs. 8 and 9; this yields $d\sigma_{992}/d\Omega = 3.5\times10^{-29}$ cm^2 sterad^{-1} molecule^{-1} (parallel polarized component; 488 nm excitation).

We now turn to the question of the relationship between the scattering cross section of water and the absolute quantum yield of a chromophore embedded in a water solvent. Within the sample medium we consider the thin cylindrical sample volume which is irradiated by the laser beam. We let l represent the length of the segment which is focused onto the detector photocathode. We let x represent an arbitrary point in this segment along the direction of light propagation ($x=0$ is the beginning of the segment and $x=l$ is the end of the segment). We denote the solid angle of detection at x by $\Omega(x)$. The intensity of the laser radiation at x is found from Beer's law:

$$I(x) = I_0 e^{-\alpha x} , \tag{1}$$

where I_0 is the intensity at the point $x=0$ and α is the absorptivity of the sample. The fluorescence intensity arriving at the photocathode from a thin slice of sample of thickness dx is simply

$$dI_f = \Phi_f \frac{\Omega(x)}{4\pi} dI(x) , \tag{2}$$

where $dI(x)$ is the amount of light absorbed by the thin slice of sample and Φ_f is the quantum yield of the sample. The factor of 4π arises from the fact that the total emission is dispersed over the entire 4π of solid angle; $\Omega(x)/4\pi$ is thus the fraction of the emitted intensity that is collected by the optics and detected. Equation (2) obviously assumes an isotropic emission pattern which is a good assumption as long as the active chromophores have time to randomly reorient before emitting light. For systems which have very short lifetimes this can be a poor approximation. Fortunately, the deviations from Eq. (2) are small for planar molecules which have two nearly equivalent absorption/emission dipoles oriented perpendicular to each other in the plane of the molecule. The heme group of cytochrome c is an example of such a situation. Given that a molecule of this type is stationary during the absorption/emission process, it is straightforward to show that, for emission at 90° to the incident photon direction and polarization, the intensity will be only 1.125 times larger than would be expected for the isotropic case. We thus continue with Eq. (2) and apply corrections due to nonisotropic emission, when needed later in the text.

Using Eqs. (1) and (2) and integrating over the entire sample segment, we find for the emission intensity

$$I_f = \Phi_f \frac{\alpha}{4\pi} \left[I_0 \int_0^l \Omega(x) e^{-\alpha x} \, dx \right]. \tag{3}$$

On the other hand, the Raman scattering intensity of the water molecules in slice dx is determined by the scattering cross section and by the absolute intensity of the light at point x (not the amount absorbed); thus,

TABLE I. The values for the Raman scattering cross section of water measured in this study. For convenience, the values for S_λ are also tabulated [see Eq. (7)]. The quantity $\tilde{\nu}_s$ is the frequency of the scattered light.

λ_0 (nm)	$\tilde{\nu}_s$ (kK)	$\frac{d\sigma_w}{d\Omega}$ (cm^2 $sterad^{-1}$ $molecule^{-1}$)	S_λ (cm)
515	16.14	8.9×10^{-30}	6.15×10^5
488	17.19	11.8×10^{-30}	4.64×10^5
458	18.54	16.6×10^{-30}	3.30×10^5

$$dI_w = I(x)\frac{d\sigma_w}{d\Omega}\Omega(x)N_w\,dx\ , \tag{4}$$

where N_w is the number of water molecules per cm^3 ($N_w\,dx$ is the number of scattering centers/unit area). Integration of Eq. (4) yields

$$I_w = \frac{d\sigma_w}{d\Omega}N_w\left[I_0\int_0^l \Omega(x)e^{-\alpha x}\,dx\right]\ . \tag{5}$$

We now define a ratio $Q \equiv I_f/I_w$ and notice that the expresssions in brackets cancel identically so that

$$\frac{I_f}{I_w} = Q = \frac{\Phi_f\alpha}{4\pi N_w(d\sigma_w/d\Omega)}\ . \tag{6}$$

Q and α are the measured experimental quantities and, along with the properties of water, they serve to determine Φ_f, the quantum yield. In terms of the extinction coefficient at the excitation wavelength, we can cast Eq. (6) into the following useful form:

$$\frac{Q}{\Phi_f\epsilon c} = \frac{2.303}{4\pi N_w(d\sigma_w/d\Omega)} \equiv S_\lambda\ , \tag{7}$$

where c is the concentration of chromophore and ϵ is the extinction coefficient at the excitation wavelength. The quantity defined as S_λ is wavelength dependent due to the fact that the scattering cross section of water is not constant, but in fact varies with the usual ν_s^4 behavior as well as with a possible additional frequency dependence. The quantities $d\sigma_w/d\Omega$ and S_λ are given in Table I for some typical laser wavelengths. The values of $d\sigma_w/d\Omega$ at other than 488 nm excitation are obtained by referencing the scattering intensity of water to an internal $SO_4^=$ standard as well as to the 3060 cm^{-1} line of benzene.

A variety of work has been reported on the absorption properties of water throughout the visible region.[10] Hulburt has measured the absorption coefficient (α_w) in the 400–700 nm range taking into account the Rayleigh scattering which is competitive with the absorption for α_w on the order of 10^{-4} cm^{-1}. His results are reproduced in graphical form in Fig. 1 and plotted along with the $d\sigma_w/d\Omega$ values we have observed in this study. It is clear that with red or deep blue excitation wavelengths one must take care to obtain the appropriate value of $d\sigma_w/d\Omega$ before applying this method. The rapidly changing absorption coefficient suggests that resonance behavior in the scattering cross section of water might take place in the red or the ultraviolet.

III. RESULTS

A. Sodium fluorescein

A simple experiment that serves both as a check of Eq. (7) and as an alternative method for the determination of $d\sigma_w/d\Omega$ is carried out by using a sample having a known quantum yield. We choose sodium fluorescein in 0.1N NaOH as our "standard" system and perform a variety of independent experiments with 488 nm excitation on dilute samples having ϵc values in the range 10^{-6} to 10^{-3} cm^{-1} (concentrations 10^{-11} to $10^{-8}M$). Under dilute conditions ($\sim10^{-5}M$) fluorescein is known to have a fluorescence quantum yield $\Phi_f = 0.9$.[11] A typical spectral emission is displayed in Fig. 2. Photobleaching effects are largely eliminated by the stirring technique as evidenced by sequential experiments on the same sample. In Fig. 3 we plot the results of our experiments as a function of the optical density of the samples. The slight concentration dependence of $Q/\Phi_f\epsilon c$ indicates a slow decrease of Q at higher concentrations which suggests that the quantum yield is decreasing. Probably

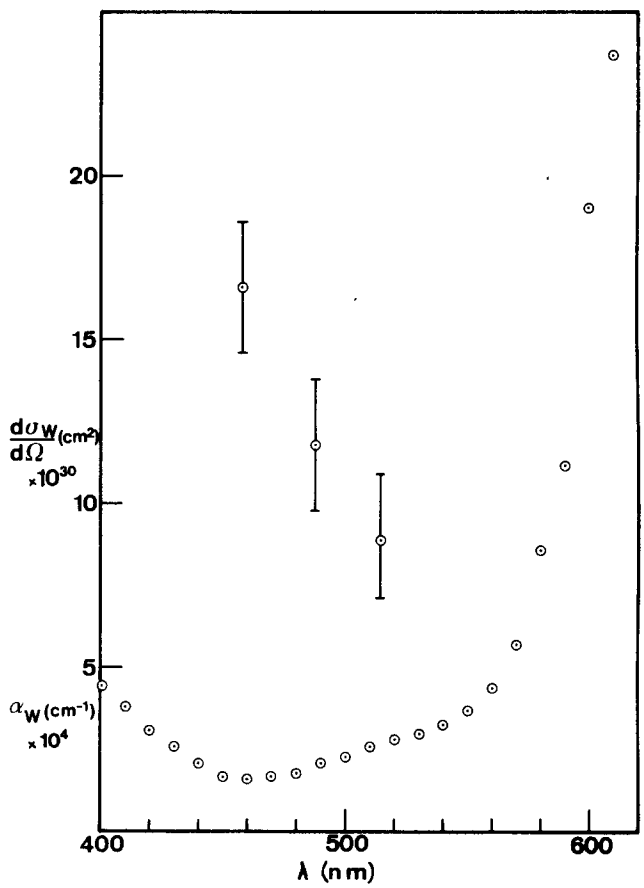

FIG. 1. The absorption coefficient of water (small circles) throughout the visible is displayed versus wavelength (from Ref. 10). The Rayleigh scattering contribution has been removed. The rapid increase of absorption in the red and the ultraviolet (not shown) suggests that care must be exercised in these regions when using the technique described in the text. The scattering cross section of water (cm^2 $sterad^{-1}$ $molecule^{-1}$) is also displayed at the three laser wavelengths employed in this study. The large error bars reflect uncertainty in the absolute value of $d\sigma_w/d\Omega$; the relative magnitudes of the three data points have much smaller errors.

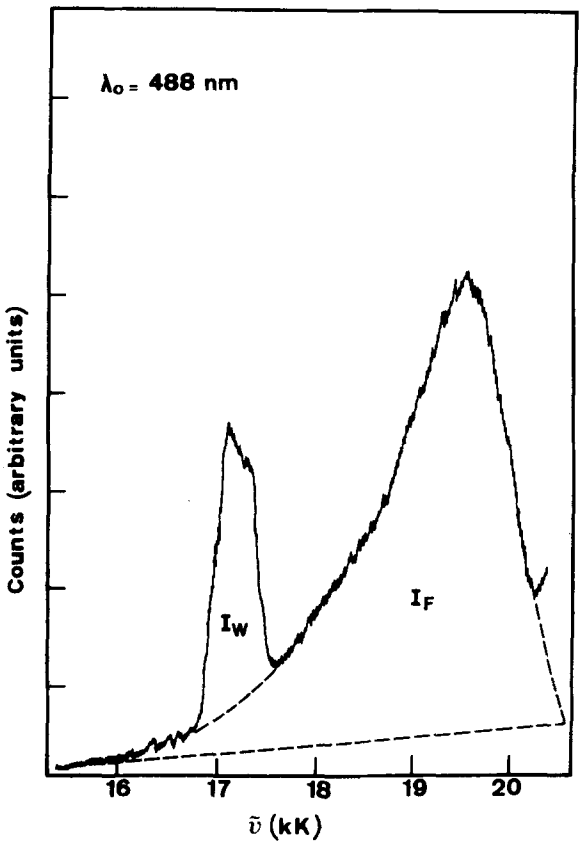

FIG. 2. A typical spectrum of sodium fluorescein in 0.1*N* NaOH. The laser excitation wavelength is 488 nm with power attenuated to 5–10 mW. The sample is constantly stirred with a small stir bar to prevent photobleaching. Sequential spectra taken on the same sample show an approximately 5%–10% decrease in I_f during the 15–30 min data accumulation time. The spectrum shown here is uncorrected for system response and the dotted line shows the base line determined by a spectrum of 0.1*N* NaOH taken just prior to the addition of the sodium fluorescein stock solution.

some weak impurity quenching or self-quenching is taking place as we approach higher concentrations. In general, the results are in quite good agreement with Eq. (7). The two dotted horizontal lines represent S_{488} obtained by using Kondilenko's[7] value for $d\sigma_w/d\Omega$ and by using our measured value. Our results are self-consistent and we therefore use $S_{488}=4.6\times10^5$ cm in the remainder of this work.

The small discrepancy between our value for $d\sigma_w/d\Omega$ and that of Kondilenko is probably due to a slight error in the system response calibration by one of us, or else due to small changes in the solid angle of detection or response which are introduced by the use of neutral density filters in Ref. 7.

We should remark that we also tried a variety of similar experiments at 488 nm excitation using the dye rhodamine 6G (Kodak). In aqueous solvents the observed values of $Q/\Phi_f\epsilon c$ are found to be lower than 4.6×10^5 cm by approximately a factor of 2. We do not understand this effect, but it could be explained by impurity quenching or by a bleaching phenomenon that may be operative in aqueous rhodamine samples at very low concentrations.[12] Samples of rhodamine prepared in ethanol give results that are in reasonable agreement with Eq. (7).

B. Flavin adenine dinucleotide

As a second check of our method we measure the quantum yield of dilute solutions of FAD (*p*H 7.0). The ϵc value of the FAD samples at the 458 nm excitation wavelength is in the range 10^{-3}–10^{-4} cm^{-1}. This corresponds to concentrations on the order of 10^{-7}–10^{-8} *M*. In Fig. 4 we display a typical (uncorrected) emission pattern for the FAD system. Using the value for S_{458} found in Table I and the measured values of Q and ϵc (2.4 and 3.4×10^{-4} cm^{-1}, respectively, for this sample), we use Eq. (7) to calculate the quantum yield. We find that $\Phi_{FAD}=0.023$ for all samples studied (to within 10%–15%). This is in very good agreement with determinations using standard techniques.[13,14]

C. Cytochrome c

In Fig. 5 we display the results of a typical experiment on ferrocytochrome c. The laser excitation wavelength is 514.5 nm, which falls within the 0–1 absorption manifold of the first excited electronic state (com-

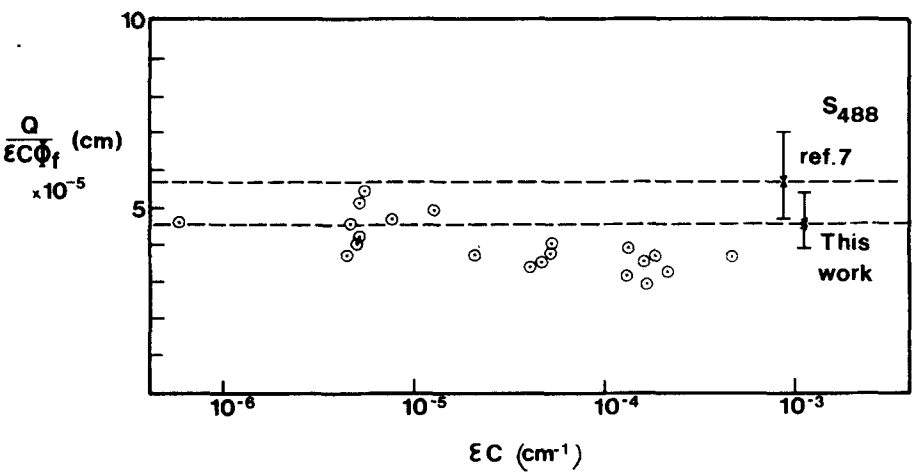

FIG. 3. A plot of $Q/\epsilon c\Phi$ versus ϵc for a variety of sodium fluorescein samples [see Eq. (7)]. The dotted lines show the value of S_{488} calculated from Kondilinko's value of the cross section (upper) and that calculated from our measured value of the cross section (lower). Our value of S_{488} agrees favorably with the fluorescence intensity of fluorescein using Eq. (7). The low values of some of the data points may be due to small photobleaching effects or weak fluorescence quenching at higher concentrations.

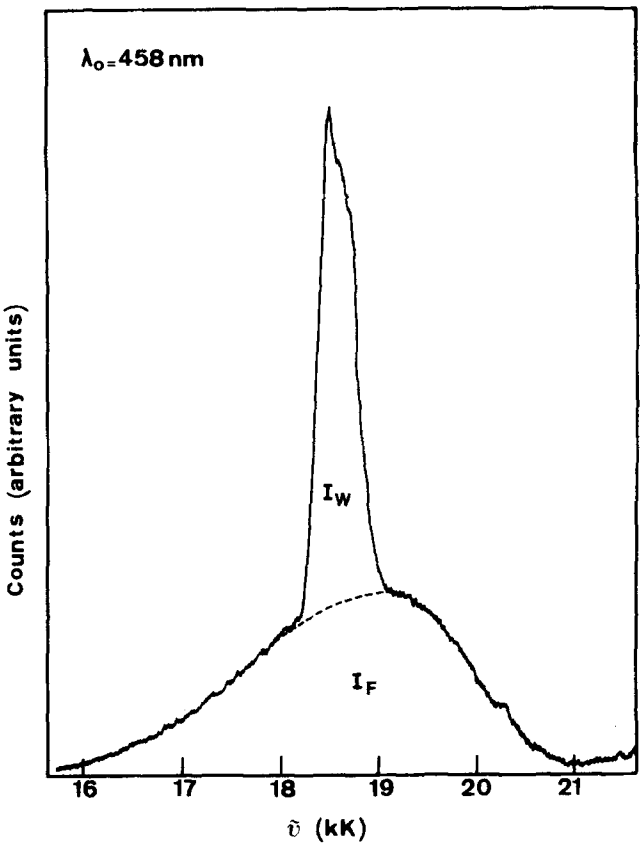

FIG. 4. A typical emission spectrum of a FAD sample using 458 nm laser excitation. The sample is stirred as in Fig. 2 and the laser power is ~ 50 mW. Sequential spectra agains reveal an approximately 5%–10% decrease in I_f during a period of 15–30 min in the laser beam. The spectrum shown here is uncorrected for system response.

monly called the β band). The broad emission from this system is, to a close approximation, a mirror image of the absorption band shape. The emission maximum at ~18.2 kK corresponds to the 0–0 absorption maximum (commonly called the α band) of the ferrocytochrome. The very narrow intense peaks found between 19.2 and 17.5 kK are the resonance Raman scattering of heme group fundamentals; between 17.5 and 16.5 kK the overtone and combination scattering is observed as sharp spikes with weaker intensity. The broad band at 16.2 kK is the Raman scattering of water. An experiment performed under identical conditions, except with the sample in the oxidized state (ferricytochrome), shows no broad band emission; only resonance Raman scattering of the heme group is observed.

Using the value for S_{515} found in Table I along with the measured values of ϵc and Q, we again use Eq. (7) to calculate the quantum yield. After averaging together the results of several different experiments and correcting for the anisotropy of the emission (see Sec. II.B), we find $\Phi_{cc} = 3.6 \times 10^{-6}$, which is quite close to the value ($\sim 4 \times 10^{-6}$) found for the emission from cytochrome B_5[5] using traditional techniques. We estimate that the errors in our determination of Φ are in the 10%–15% range Similar measurements using 520.8 nm excitation yield $\Phi_{cc} = 3.2 \times 10^{-6}$.

IV. INTERPRETATION

When the emission quantum yields become very small, as in the case of cytochrome c, we must recognize that several different emission channels may be active. Here we wish to consider the following three radiative processes: (1) resonance Raman (Rayleigh) scattering, (2) resonance fluorescence, (3) relaxed fluorescence. Resonance scattering is often easy to differentiate from processes (2) and (3) because of the different linewidths associated with the coherent (sharp) scattering process versus the incoherent (broad) emission processes. On the other hand, the differentiation of processes (2) and (3) (in the frequency domain) can be much more difficult, if not impossible. However, it is possible to consider limiting cases (such as dye molecules or FAD) which have large quantum yields that are dominated by relaxed fluorescence. In these cases it is a reasonably straightforward excercise to obtain information about the excited state lifetime from a determination of the quantum yield.[15] The purpose of this section is to present a simple kinetic model which allows us to take into account all three processes mentioned above and to discuss some limiting cases of the model in the low quantum yield limit.

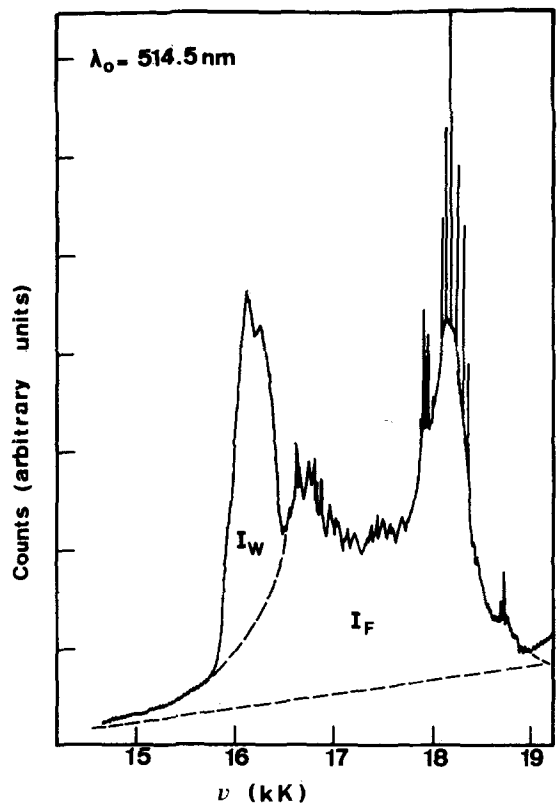

FIG. 5. A typical emission spectrum of ferrocytochrome c using 514.5 nm excitation. The optical density of this sample is 1.02 at the excitation wavelength (1 cm path length). The sample is stirred as before, although no time dependent photoeffects are observed. The laser power is 100 mW. The very narrow spikes are resonance Raman scattering from the heme group. The spectrum shown here is not corrected for system response. The base line is given by the dotted line and is determined by a buffer blank taken just prior to this spectrum.

A. Quantum mechanical treatement

We begin with a brief review of the quantum mechanical treatment of the spectral re-emission [resonance Raman (Rayleigh) scattering and resonance fluorescence] in a simple three state system undergoing collisions in the impact approximation.[16,17] This subject has been a topic of current interest and detailed accounts can be found in the literature.[18–21] We let $dW/d\omega_s$ be the rate of photon counts in the frequency range ω_s to $\omega_s + d\omega_s$ so that we can express the spectral distribution of resonance scattering and resonance fluorescence as

$$\frac{dW}{d\omega_s} = \frac{d\sigma(\omega_0, \omega_s)}{d\omega_s} K_0 \,. \tag{8}$$

Here K_0 is the incident flux (number photons/cm^2 sec) and $d\sigma/d\omega_s$ is the cross section, given in the three state model by

$$\frac{d\sigma}{d\omega_s} = \frac{8\pi\omega_s^3\omega_0}{9c^4} \frac{|\langle f|R|i\rangle|^2 |\langle i|R|g\rangle|^2}{(\hbar\omega_0 - E_{gi})^2 + (\Gamma_T/2)^2} \times \left[\delta(\omega_0 - \omega_s - \omega_{fg}) + \frac{\hbar\Gamma_{pc}}{\pi\Gamma_i} \frac{\Gamma_T/2}{(\hbar\omega_s - E_{if})^2 + (\Gamma_T/2)^2}\right]. \tag{9}$$

Figure 6 schematically represents the ground (g), intermediate (i), and final (f) states of the three state system; the energy separations between the states are noted as E_{gi} and E_{if}. The frequencies ω_0 and ω_s correspond to the incident and scattered/emitted frequency, respectively; while ω_{fg} corresponds to the frequency of the Stokes shift between states g and f. The quantities $\langle i|R|g\rangle$ and $\langle f|R|i\rangle$ are the absorption and emission dipole matrix elements and Γ_T is the homogeneous broadening (FWHM) associated with state i (all the Γ's will be defined in detail below). It is easy to see that the first term in curly brackets represents the spectral contribution from resonance Raman scattering (it is sharp and tracks with ω_0), whereas the second term results from resonance fluorescence (it is broad, taking the excited state width, and remains at a fixed frequency E_{if} independent of ω_0).

The meaning of the various Γ's in Eq. (9) can be ascertained by consideration of Fig. 6 (see also Ref. 3) and is related to the more formal optical dephasing times[22] T_1, T_2, and T_2'. Given that the ground electronic state does not undergo inelastic transitions between molecular levels (i.e., infinite T_1 in the ground electronic state), we obtain the usual equation for total dephasing of the excited state[22,23]:

$$\frac{2}{T_2} = \frac{1}{T_1} + \frac{2}{T_2'} \,, \tag{10}$$

where $2\hbar/T_2 \equiv \Gamma_T$ is the total homogeneous broadening (FWHM) for the transition $g \rightarrow i$.[22] The explicit notation is as follows:

$$\Gamma_T = \Gamma_i + \Gamma_{pc}, \quad \Gamma_i \equiv \frac{\hbar}{T_1} = \Gamma_e + \Gamma_v + \Gamma_r, \quad \Gamma_{pc} \equiv \frac{2\hbar}{T_2'} \,, \tag{11}$$

where Γ_i is the broadening of state i from inelastic processes such as radiative decay (Γ_r), intramanifold vibrational decay (Γ_v), and extramanifold nonradiative decay (Γ_e). The quantity Γ_{pc} represents the line broadening due to quasielastic phase changing processes which occur between the ground and excited state and reflect a disparity in the elastic scattering amplitudes of the two states.[22]

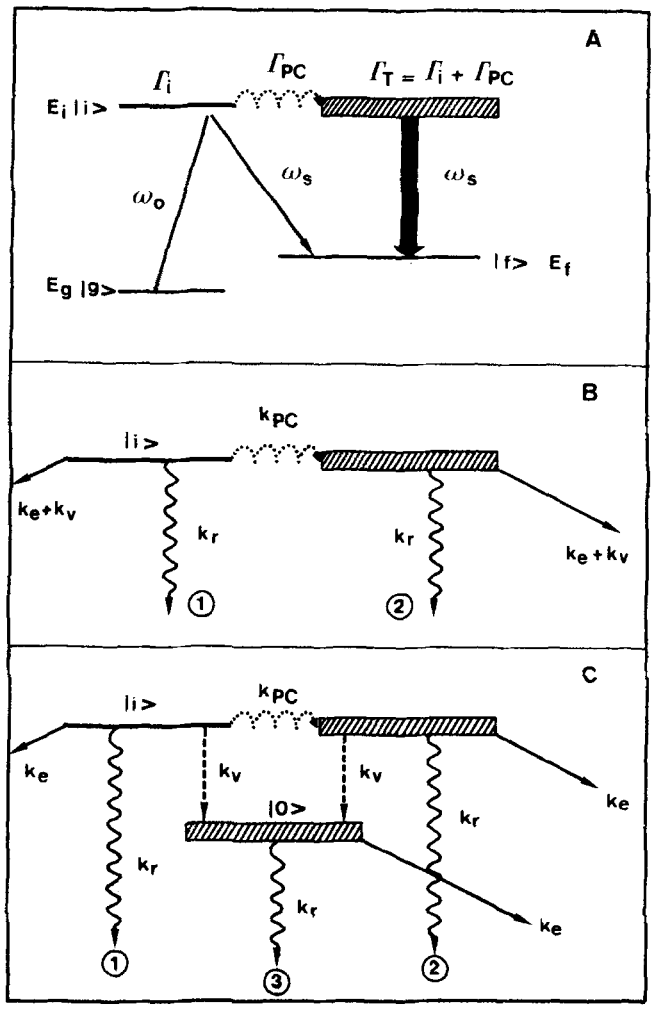

FIG. 6. (A) A schematic diagram of the spectral re-emission in the three state model. The incident laser frequency is ω_0 and the frequency of the coherent scattering is given by $\omega_s = \omega_0 - \omega_{fg}$, where $\hbar\omega_{fg} = E_f - E_g$. The incoherent emission, which takes the width of the excited state i by means of the dephasing process, is independent of the laser frequency. A unified treatment of the spectral re-emission considers the coherent and incoherent components simultaneously; thus, the quantity ω_s plays the variable role of the frequency of resonance fluorescence and the frequency of resonance scattering [see Eq. (9)]. (B) A simple kinetic picture showing the two routes of re-emission from state i. Process (1) corresponds to resonance Raman scattering; process (2) corresponds to resonance fluorescence. The nonradiative decay rate is given as $k_e + k_v$. The phase changing rate is described by k_{pc} and the radiative rate is k_r. (C) Same as (B) except that a relaxed emitting state is added to the picture. Process (3) corresponds to relaxed fluorescence. Now the intramanifold nonradiative vibrational decay takes state i into state 0 with a rate k_v. The extramanifold nonradiative decay rate is k_e.

Since both terms in Eq. (9) are sharply peaked with respect to the incident or scattered (visible) light frequencies, we can integrate over ω_s and identify the amount of light scattered into state f via the Raman channel as well as the amount of light emitted as resonance fluorescence into state f. The result is

$$W_R^f = \frac{8\pi\omega_s^3\omega_0}{9c^4}\,\frac{|\langle f|R|i\rangle|^2|\langle i|R|g\rangle|^2}{(\hbar\omega_0 - E_{gi})^2 + (\Gamma_T/2)^2}K_0\,,$$

$$W_F^f = \frac{8\pi\omega_s^3\omega_0}{9c^4}\,\frac{|\langle f|R|i\rangle|^2|\langle i|R|g\rangle|^2}{(\hbar\omega_0 - E_{gi})^2 + (\Gamma_T/2)^2}\,\frac{\Gamma_{pc}}{\Gamma_i}K_0\,, \qquad (12)$$

where we see immediately that the balance between resonance Raman and resonance fluorescence is simply $W_F^f/W_R^f = \Gamma_{pc}/\Gamma_i$ as discussed previously.[18-21]

If we now take advantage of the simplicity of the single excited state model, we can sum over final states term by term (including the $f = g$ Rayleigh term) and identify the standard expression for the radiative lifetime[15]

$$\frac{1}{\tau_r} = \frac{8\pi\omega_s^3}{3\hbar c^3}\sum_f |\langle i|R|f\rangle|^2 = \frac{\Gamma_r}{\hbar}\,, \qquad (13)$$

so for the total light emission we have ($W = \sum_f W^f$)

$$W_R = \frac{2\pi\omega_0}{3c}\,\frac{|\langle i|R|g\rangle|^2}{(\hbar\omega_0 - E_{gi})^2 + (\Gamma_T/2)^2}\,\Gamma_r K_0\,,$$

$$W_F = \frac{2\pi\omega_0}{3c}\,\frac{|\langle i|R|g\rangle|^2}{(\hbar\omega_0 - E_{gi})^2 + (\Gamma_T/2)^2}\,\frac{\Gamma_r\Gamma_{pc}}{\Gamma_i}K_0\,, \qquad (14)$$

and finally, by straightforward application of the golden rule, we calculate the rate of absorption of photons for the transition g to i:

$$W_{abs} = \frac{2\pi\omega_0}{3c}\,\frac{|\langle i|R|g\rangle|^2\Gamma_T}{(\hbar\omega_0 - E_{gi})^2 + (\Gamma_T/2)^2}K_0\,, \qquad (15)$$

so that, within the assumptions of the simple three state model,

$$W_R = \frac{\Gamma_r}{\Gamma_T}W_{abs}\,, \quad W_F = \frac{\Gamma_r\Gamma_{pc}}{\Gamma_i\Gamma_T}W_{abs}\,. \qquad (16)$$

B. Kinetic treatment

It is interesting at this point to turn to a simple kinetic picture of the excited state i. We define our rate constants in the usual way:

$$\frac{1}{\tau} = k \equiv \frac{\Gamma}{\hbar}\,, \qquad (17)$$

and in Fig. 6(B) we illustrate a schematic diagram for the evolution of state i in terms of the rate constants k_r, k_{pc}, k_e, and k_v. Radiative process (1) corresponds to the coherent scattering which is sharp and has not taken on the width of state i, whereas radiative process (2) corresponds to the incoherent emission (resonance fluorescence) which is broad and takes the full width of state i. A kinetic analysis for the yields via channels (1) and (2) gives [using Eq. (11)]

$$Y_1 = \frac{\Gamma_r}{\Gamma_T} = \frac{\tau_i}{\tau_r}\left(\frac{1}{1+\tau_i/\tau_{pc}}\right)\,,$$

$$Y_2 = \frac{\Gamma_{pc}\Gamma_r}{\Gamma_T\Gamma_i} = \frac{\tau_i}{\tau_r}\left(\frac{1}{1+\tau_{pc}/\tau_i}\right)\,, \qquad (18)$$

which as must be expected is the same as the quantum mechanical result [Eq. (16)].

We now expand the kinetic picture to include an additional relaxed emitting state $|0\rangle$. This state corresponds to the ground vibrational state in the excited state manifold and emission from this state is called relaxed fluorescence. Figure 6(C) shows the kinetic scheme. The yields for processes (1) and (2) are the same as in Eq. (18) but in addition we obtain the expression for the relaxed yield [process (3)]

$$Y_3 = \frac{\Gamma_v\Gamma_r}{\Gamma_i(\Gamma_r+\Gamma_e)} = \frac{\tau_i}{\tau_r}\left(\frac{1/\tau_v}{1/\tau_r + 1/\tau_e}\right)\,. \qquad (19)$$

We next consider some limiting cases of Eqs. (18) and (19) by recalling that τ_r is typically on a nanosecond time scale whereas τ_v is typically on the order of picoseconds. If we first consider τ_e to be very long (on the order of τ_r or longer), we find from Eq. (19) the expression appropriate for large quantum yield systems[15]:

$$Y_3 = \frac{1}{1+\tau_r/\tau_e}\,, \quad \tau_r,\ \tau_e \gg \tau_v\,. \qquad (20)$$

Processes (1) and (2) are clearly much weaker than the relaxed emission in this limit and are scaling with the factor $\tau_v/\tau_r \sim 10^{-3}$. Since we are concerned here with the small quantum yield limit, we must obviously consider the effect of making τ_e much smaller than τ_r. In this limit the relaxed yield becomes [from Eq. (19)]

$$Y_3 = \frac{\tau_e}{\tau_r}\left(\frac{1}{1+\tau_v/\tau_e}\right)\,. \qquad (21)$$

In Fig. 7(A) we plot Y_3 in this limit as a function of τ_v/τ_e with the magnitude of Y_3 expressed in units of τ_e/τ_r. This is a useful diagram because it suggests that we consider three separate regions as τ_e varies with respect to τ_v. We select the three following cases for detailed consideration:

$\tau_e \gg \tau_v$ ($\tau_e \ll \tau_r$), case I,

$\tau_e = \tau_v$ ($\tau_e \ll \tau_r$), case II,

$\tau_e \ll \tau_v$ ($\tau_e \ll \tau_r$), case III.

1. Case I

Under the conditions of case I we have the following limits for the three radiative processes under discussion:

$$Y_1 = \frac{\tau_v}{\tau_r}\left(\frac{1}{1+\tau_v/\tau_{pc}}\right)\,,$$

$$Y_2 = \frac{\tau_v}{\tau_r}\left(\frac{1}{1+\tau_{pc}/\tau_v}\right)\,,$$

$$Y_3 = \frac{\tau_v}{\tau_r}\cdot\frac{\tau_e}{\tau_v}\,. \qquad (22)$$

Plots of the relative strengths (in units of τ_v/τ_r) of the three processes as a function of τ_{pc}/τ_v are found in Fig. 7(B). Notice that the relaxed emission (Y_3) is still the dominant process and is independent of the rate of dephasing. For case I, the relaxed emission is typically a factor of τ_e/τ_v times larger than the resonance scattering or resonance fluorescence.

2. Case II

When case II conditions are implemented the intensity of the relaxed emission drops into the range of processes (1) and (2). The expressions for the yields take the following forms:

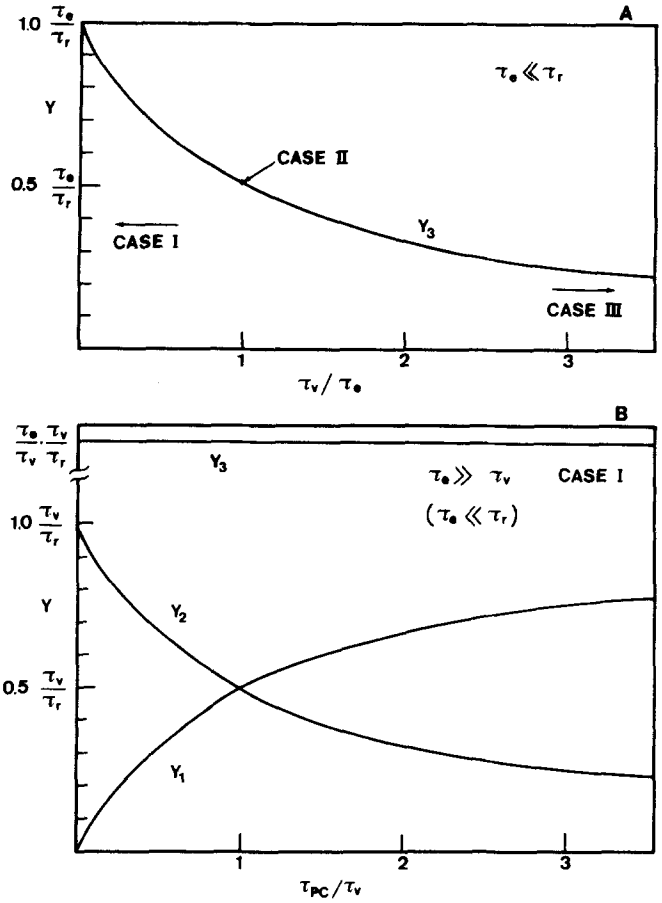

FIG. 7. (A) A plot of the relaxed fluorescence Y_3 as a function of τ_v/τ_e in the limit $\tau_e \ll \tau_r$ [see Eq. (21)]. We select three cases representative of a wide range of values for τ_e. Case I is defined by $\tau_v/\tau_e \ll 1$, case II is defined by $\tau_v/\tau_e = 1$, and case III is defined by $\tau_v/\tau_e \gg 1$. The asymptotic value for Y_3 in case III is $\tau_e^2/(\tau_v \tau_r)$. (B) The emission intensities for the three processes under discussion are plotted versus τ_{pc}/τ_v in the case I limit. The yield intensities are given in units of τ_v/τ_r. Y_1 is resonance Raman scattering, Y_2 is resonance fluorescence, and Y_3 is relaxed fluorescence, the dominant process in this case.

$$Y_1 = \frac{\tau_e}{2\tau_r}\left[\frac{1}{1+\tau_e/(2\tau_{pc})}\right],$$

$$Y_2 = \frac{\tau_e}{2\tau_r}\left(\frac{1}{1+2\tau_{pc}/\tau_e}\right),$$

$$Y_3 = \frac{\tau_e}{2\tau_r}. \qquad (23)$$

Plots of the relative strengths of the three processes are found in Fig. 8(A), where we plot the yields (in units of τ_e/τ_r) versus τ_{pc}/τ_e. Notice that the maximum of total incoherent emission ($Y_2 + Y_3$) is found at $\tau_{pc}/\tau_e = 0$ and is equal to τ_e/τ_r. Moreover, when $\tau_{pc}/\tau_e \gtrsim \frac{1}{2}$ it appears that the resonance scattering process is competitive with the relaxed fluorescence and will be observed.

3. Case III

Finally, we turn to case III conditions and find that the relaxed yield drops below that for resonance scattering and resonance fluorescence. The expressions (18) and (19) take the following form:

$$Y_1 = \frac{\tau_e}{\tau_r}\left(\frac{1}{1+\tau_e/\tau_{pc}}\right),$$

$$Y_2 = \frac{\tau_e}{\tau_r}\left(\frac{1}{1+\tau_{pc}/\tau_e}\right),$$

$$Y_3 = \frac{\tau_e}{\tau_r} \cdot \frac{\tau_e}{\tau_v}. \qquad (24)$$

Plots are found in Fig. 8(B) with yield in units of τ_e/τ_r displayed versus τ_{pc}/τ_e. Again the maximum of total incoherent emission is found at $\tau_{pc}/\tau_e = 0$ and in this case the yield is primarily due to resonance fluorescence (Y_2). The maximum value is again seen to be approximately equal to τ_e/τ_r. In case III, with $\tau_{pc}/\tau_e \gtrsim 2$, resonance scattering clearly becomes the dominant radiative process.

V. DISCUSSION

It is important to realize that large chromophores are very complicated systems and that the simple one or two excited state model presented here is only a schematic representation of the real system. This is especially true in the derivation of Eq. (16). The sum over

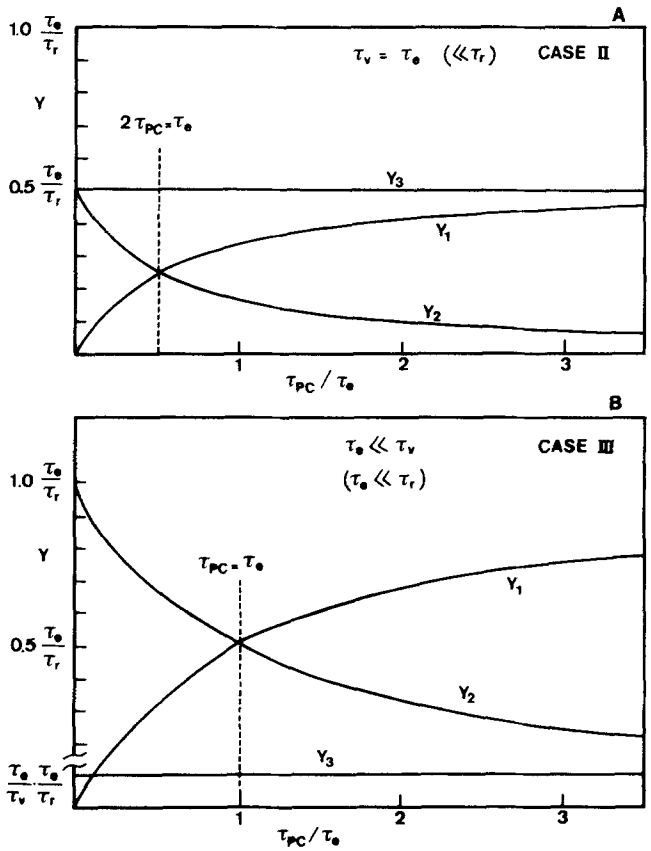

FIG. 8. (A) A plot of the yield intensities in the case II limit. The vertical dotted line locates the point $\Gamma_i = \Gamma_{pc}$ which corresponds to an equal balance between resonance fluorescence and resonance Raman scattering. All three processes are competitive in this case. Notice that, as τ_{pc}/τ_e increases, resonance Raman and relaxed fluorescence become dominant. (B) Same as above except in case III limit. Notice that relaxed fluorescence is diminished in this case and that at large τ_{pc}/τ_e resonance Raman scattering is the dominant process.

intermediate states, which is one of the main difficulties in the evaluation of the Kramers–Heisenberg dispersion equation,[2,24] is completely eliminated by consideration of only a single excited state. Nevertheless, by use of the simple model presented, we can quantitate the incoherent emission within a logical framework that allows us to obtain information about the excited state lifetimes and the magnitude of the damping factor (Γ_T). A reasonable estimation is clearly important for the calculation of Raman excitation profiles[2] and absorption band shapes.[24]

We also wish to note that a much more detailed analysis of light emission from a thermally relaxing multilevel system has been previously presented by Mukamel and Nitzan.[25] Our simple kinetic scheme must certainly be a limiting case of their more formal theory. Unfortunately, the complexity of their very general approach makes its application difficult if more than two or three levels are included.[25] As a result, we have turned to the simple kinetic analysis in order to obtain estimates of the various contributions to the total damping factor; our analysis is clearly an approximation and should not be considered capable of providing precise results.

A. Fluorescein and FAD

The quantum yield measurements presented in Sec. III provide some interesting examples of the various cases discussed in the previous section. Sodium fluorescein, which has a quantum yield near unity, is obviously described in the limit τ_r, $\tau_e \gg \tau_v$ and Eq. (20) gives the relationship between the (dominant) relaxed fluorescence, the radiative rate ($1/\tau_r$), and the extra-manifold nonradiative rate ($1/\tau_e$). For the case of sodium fluorescein $Y_3 = 0.9$ which, using Eq. (20), implies $\tau_e \simeq 10\tau_r$. Thus, the Strickler–Berg relation[15] can be applied to the electronic absorption band of fluorescein to yield τ_r and τ_e [or, using Eq. (17), Γ_r and Γ_e]. Unfortunately, an estimation of the damping factor Γ_T is not facilitated in this case since Γ_r, $\Gamma_e \ll \Gamma_v$, Γ_{pc} [see Eqs. (11) and (17)] and Γ_T is determined primarily by Γ_v and Γ_{pc}. In principle, a reasonable estimate of Γ_v and Γ_{pc} can be obtained from a careful Raman linewidth analysis,[26–28] since in real systems the final state f has its homogeneous linewidth determined primarily by vibrational relaxation and pure dephasing. For room temperature liquids, typical estimates for the vibrational relaxation and the dephasing rate are on the order of picoseconds[29]; such estimates would indicate a Γ_T on the order of 5–25 cm^{-1} for molecules like sodium fluorescein. The broad asymmetric characteristics of the absorption band (width ~1.5–2.0 kK) are presumably accounted for by a combination of inhomogeneous broadening, sequence broadening, and Franck–Condon effects in the strong and/or weak coupling limit.[24]

The FAD sample has a somewhat smaller quantum yield (0.023), but the dominant emission process is still relaxed fluorescence. In fact, the FAD system illustrates some of the difficulties that can be encountered when relating quantum yield measurements to the excited state lifetime. Weber has shown that FAD in solution actually exists in two forms in dynamic equilibrium.[13,30] The "closed" form is occupied by approximately 90% of the FAD molecules and has a very low quantum yield. The "open" form is occupied by the remaining 10% of the FAD molecules and has a quantum yield very close to that of the pure flavine molecule (isoalloxazine) $\Phi_{FMN} = 0.25$. Thus, our spectrum in Fig. 4 is really a superposition of the emission from the two species, with the weak emission from the closed form essentially undetectable due to the strong fluorescence of the open form. Without the additional direct lifetime measurements which uncover these internal quenching effects, one might mistakenly classify FAD as a case I complex and, as a result, calculate τ_e incorrectly. Clearly, the open form of FAD has its damping factor determined primarily by Γ_v and Γ_{pc} as in the case of sodium fluorescein. The closed form, on the other hand, is a very low quantum yield system and not much can be deduced about the Γ_T of this complex unless it can be studied independently from the open form.

B. Cytochrome c

Cytochrome c provides us with the most interesting example of a low quantum yield system. The total incoherent yield ($Y_2 + Y_3$) of the ferrocytochrome is measured to be 3.6×10^{-6} but no broad band emission from the ferricytochrome is detected (only resonance Raman scattering is observed). Clearly, the ferric cytochrome is an example of a case III system with $\tau_{pc}/\tau_e \gg 1$ [see Fig. 8(B)]. The absence of any detectable incoherent emission in the ferric system again complicates the quantitation of Γ_T but it is possible to conclude that $\tau_e(\text{ferric}) \ll \tau_e(\text{ferrous})$ assuming that τ_v and τ_{pc} are insensitive to the change in valence of the heme iron atom. In both valence states of cytochrome c, Γ_e plays a much more important role in the determination of Γ_T than in the previous examples and we can expect that Γ_T is substantially larger than 5 cm^{-1} for the cytochrome c system.

Since intense resonance Raman scattering as well as incoherent emission is observed in the ferrocytochrome, we must classify this system as either a case III or case II example. In either case (as well as for case I) the maximum yield of incoherent emission (in limit as $\tau_{pc}/\tau_e \to 0$) places a minimum value on τ_e. A Strickler–Berg calculation gives $\tau_r = 5\times10^{-8}$ sec for the α–β band of ferrocytochrome so that $\tau_e^{min} = 0.18$ psec. From the work of Friedman and Rousseau,[3] however, we know that the balance between resonance Raman and resonance fluorescence in this compound is strongly influenced by lowering the temperature (τ_{pc} increases at low temperature and the resonance fluorescence disappears). Friedman and Rousseau conclude that $\Gamma_{pc} \simeq \Gamma_i$ in this system which seems to be a reasonable approximation. In case III this approximation leads to $\tau_{pc} \simeq \tau_e$; while in case II we have $\tau_e \simeq 2\tau_{pc}$. These values of τ_{pc}/τ_e are located in Fig. 8 by the dotted lines..

Using these values of τ_{pc}/τ_e, we can calculate the sum of the incoherent emission yield ($Y_3 + Y_2$) in either the case II or case III limit. In case II we have [see Fig. 8(A)]

$$Y_2 + Y_3 = \frac{1}{4}\frac{\tau_e}{\tau_r} + \frac{1}{2}\frac{\tau_e}{\tau_r} = 3.6\times10^{-6} ,$$

which yields $\tau_e = 0.24$ psec. With $\Gamma_e = \Gamma_v = \Gamma_{pc}/2$, we have for the total damping factor

$$\Gamma_T = 20\ \text{cm}^{-1} + 20\ \text{cm}^{-1} + 40\ \text{cm}^{-1} + 0\ \text{cm}^{-1} = 80\ \text{cm}^{-1}\ .$$
$$(\Gamma_e) \quad (\Gamma_v) \quad (\Gamma_{pc}) \quad (\Gamma_r) \quad \text{(case II)}$$

For case III the dominant incoherent emission is from Y_2 with a small fraction τ_e/τ_v (which we take as 0.1 for the calculation) coming from Y_3 [see Fig. 8(B)]. In this limit we get $\tau_e = 0.3$ psec, which, with $\Gamma_e = \Gamma_{pc} \gg \Gamma_v$, implies

$$\Gamma_T = 16.7\ \text{cm}^{-1} + 16.7\ \text{cm}^{-1} + 1.7\ \text{cm}^{-1} + 0\ \text{cm}^{-1} = 35\ \text{cm}^{-1}$$
$$(\Gamma_e) \quad (\Gamma_{pc}) \quad (\Gamma_v) \quad (\Gamma_r) \quad \text{(case III)}$$

We thus obtain an approximate value for the damping factor in the α–β region of ferrocytochrome c, consistent with the quantum yield measurement. The results of either case II or case III are compatible with experiment and are to be considered as reasonable approximations due to the uncertainty in the ratio τ_{pc}/τ_e and the simplicity of our model. We also note that the absolute maximum value of Γ_e, consistent with the quantum yield, is 30 cm^{-1}; this occurs at the extreme $\tau_{pc}/\tau_e = 0$. As τ_{pc}/τ_e increases, the Γ_e obtained from the quantum yield measurement decreases; physically reasonable values of of Γ_e are given by the case II and III examples cited above.

We should discuss at this point some of the uncertainties implicit in our determination of τ_e. Clearly, the lower limit that we set on τ_e ($\tau_e^{\min} = 0.18$ psec) is an extrapolation into a nonrealistic regime where no resonance Raman scattering is observed ($\tau_{pc}/\tau_e \to 0$, $Y_2/Y_1 \to \infty$). We find more realistic values for τ_e assuming equal amounts of resonance scattering and resonance fluorescence as discussed above and in Ref. 3. Using this assumption throughout the region between case II ($\tau_e = \tau_v$) and case III ($\tau_e \ll \tau_v$), we find that τ_e lies in the remarkably narrow range of 0.24–0.3 psec. Even if we allow for the possibility that the incoherent resonance fluorescence is larger than the resonance scattering (the data from Ref. 3 make it appear highly unlikely that the resonance fluorescence contribution is less than the resonance scattering), we see that τ_e can be decreased at most to $\tau_e^{\min}$. Thus, we take the view that τ_e lies with good certainty in the range 0.2–0.3 psec for β-band excitation.

The other components (Γ_{pc}, Γ_v) comprising the total homogeneous damping factor are seen to be less precisely determined in our analysis. This uncertainty arises in a well defined way in our model from the variation in parameters as we move from the case II to the case III limit. Until further experiments can determine with more accuracy the ratios τ_{pc}/τ_e and/or τ_v/τ_e, we must be content with the above approximations for Γ_T. (Note, $\tau_v \simeq 1$ psec $\Rightarrow \tau_v/\tau_e \simeq 4$, between case II and III.) Finally, we should add that the other small uncertainties in our calculation may arise from our use of the Strickler–Berg relationship to determine τ_r. This relationship is not well established for very weak or forbidden transitions; however, the α–β band of cytochrome c is sufficiently intense ($\epsilon_{\alpha} = 27\,000 M^{-1}\ \text{cm}^{-1}$) to fall well within the limits of applicability discussed by Strickler and Berg.

Our quantitative estimates of the excited state lifetime and damping factor in the α–β region of cytochrome c should be contrasted with the qualitative discussion in Refs. 3 and 4 which suggests that the excited state lifetime is on the order of tens of femtoseconds and indicates that the full width of the α band is due to homogeneous broadening. Although the quantum yield measurements do support the view that there is a sizeable homogeneous contribution to the line shape, these measurements also seen to rule out the possibility that homogeneous broadening alone generates the full width at room temperature.

Additional quantum yield measurements using α-band (0–0) excitation may help to more fully resolve this discrepancy. Certainly, our simple kinetic model is applicable to the case of 0–0 excitation since $\tau_v \to \infty$ for excitation into the state $|0\rangle$ [see Fig. 6(C)], placing us in the case III limit with $Y_3 \to 0$. The identical situation is discussed in Ref. 3 using the same three state model [Eq. (9)]; it should therefore be very interesting to monitor (quantitatively) the intensity of the incoherent quantum yield as the laser excitation is tuned from the β band into the α band. Obviously, a factor of 5 decrease in the quantum yield must be observed in order to indicate a τ_e of 50 psec in the α-band region. On the other hand, a more complex and complete theoretical analysis of the observed emission yields is certainly possible.[25] It seems unlikely to us, however, that any such analysis can yield excited state lifetimes significantly shorter than 0.2 psec and still account quantitatively for the light emission observed with 514.5 and 520.8 nm excitation.

The homogeneous linewidths found here are somewhat smaller than the observed width of the 0–0 transition in ferrocytochrome, which is on the order of 200 cm^{-1} at room temperature.[31] Presumably, the remaining difference in the widths is due to inhomogeneous and librational broadening effects or dimensional fluctuations[32] of the heme chromophore. A Franck–Condon/density-of-states mechanism[24] probably plays a minor role in the broadening of these transitions as evidenced by the lack of Franck–Condon active resonance Raman scattering in the α–β region.

Turning back to the ferric cytochrome, we conclude that Γ_T is increased primarily due to a decrease in τ_e. This effect is possibly due to increased interaction of the porphyrin π orbitals with the unfilled t_{2g} subshell of the ferric iron atom. The broadened absorption bands of the ferric cytochrome also attest to the larger Γ_T. Similar effects have been noted in the Soret bands (S_2) of these proteins where excitation profile measurements[2] indicate that Γ_T for the ferric protein is substantially larger than for the ferrous cytochrome.

Finally, it is important to point out that resonance Raman scattering is clearly the dominant process upon Soret band excitation of ferrocytochrome c[2]; however, weak incoherent emission also appears to be present.[33] Assuming that the pure dephasing rates (τ_{pc}) are similar for Soret and α-band excitation, any weak emission from the Soret band must be analyzed under the condition $\tau_{pc}/\tau_e \gg 1$ [i.e., see right hand side of case III, Fig.

8(B)]. Under these conditions, the observed emission yields predict damping factors (Γ_T) on the order of 200 cm^{-1} for S_2 which are almost solely determined by the extramanifold nonradiative decay (Γ_e). A detailed presentation of the Soret band emission properties will be presented in a future publication.

ACKNOWLEDGMENTS

The authors are particularly grateful to Mmes. G. Chottard and L. Tosi for making available the spectroscopic equipment used in this work, and to Mr. M. Krauzman for helpful discussions regarding the calibration of optical systems for use in absolute intensity measurements. A. C. Albrecht is especially thanked for helpful comments leading to the conception of this study. In addition, we would like to gratefully acknowledge the entire biospectroscopy group at I. B. P. C. (E. Begard, P. Debey, P. Douzou, G. Hui Bon Hoa, and D. Rigos) for their research support and bon vouloir throughout the course of this work. P.M.C. is the recipient of a NSF/CNRS exchange fellowship and is partially supported through a grant from the National Institutes of Health AM 20379.

[1]J. D. Jackson, in *Classical Electrodynamics* (Wiley, New York, 1975), 2nd edition, p. 291.
[2]P. M. Champion and A. C. Albrecht, J. Chem. Phys. **71**, 1110 (1979).
[3]J. M. Friedman and D. L. Rousseau, Chem. Phys. Lett. **55**, 488 (1978).
[4]J. M. Friedman, D. L. Rousseau, and F. Adar, Proc. Natl. Acad. Sci. (U.S.A.) **74**, 2607 (1977).
[5]F. Adar, M. Gouterman, and S. Aronowitz, J. Phys. Chem. **80**, 2184 (1976).
[6]M. Moskovits and K. H. Michaelian, J. Chem. Phys. **69**, 2306 (1978).
[7]I. I. Kondilenko, P. A. Korotkov, V. Klimenko, and O. P. Demyaneko, Opt. Spectrosc. (USSR) **43**, 384 (1977).
[8]Y. Kato and H. Takuma, J. Chem. Phys. **54**, 5398 (1971).
[9]J. G. Skinner and W. Nilsen, J. Chem. Phys. **58**, 113 (1968).
[10]E. O. Hulbert, J. Opt. Soc. Am. **35**, 698 (1945); A. Tam, Nature (London) **280**, 302 (1979).
[11]J. Olmsted, J. Phys. Chem. **83**, 2581 (1979).
[12]R. Dzhumadinov and N. Nizamov, Opt. Spectrosc. (USSR) **47**, 154 (1979).
[13]G. Weber, Biochem. J. **47**, 114 (1950).
[14]The quantum yield of FAD is taken to be (1/11)th that of flavine mononucleotide ($\Phi_{FMN} = 0.25$); G. Weber (private communication).
[15]J. B. Birks, in *Photophysics of Aromatic Molecules* (Wiley-Interscience, New York, 1970).
[16]V. Hizhnyakov and I. Tehver, Phys. Status Solidi **21**, 755 (1967).
[17]D. L. Huber, Phys. Rev. **158**, 843 (1967).
[18]D. L. Rousseau and P. F. Williams, J. Chem. Phys. **64**, 3519 (1976).
[19]R. M. Hochstrasser and F. A. Novak, Chem. Phys. Lett. **53**, 3 (1978).
[20]R. M. Hochstrasser and C. A. Nyi, J. Chem. Phys. **70**, 1112 (1979).
[21]J. M. Friedman, J. Chem. Phys. **71**, 3147 (1979).
[22]K. F. Jones and A. H. Zewail, in *Advances in Laser Chemistry* (Springer, New York, 1978), pp. 196, 258.
[23]C. P. Slichter, in *Principles of Magnetic Resonance* (Springer, New York, 1978), p. 182.
[24]P. M. Champion and A. C. Albrecht, J. Chem. Phys. **72**, 6498 (1980).
[25]S. Mukamel and A. Nitzan, J. Chem. Phys. **66**, 2462 (1977).
[26]D. W. Oxtoby and S. A. Rice, Chem. Phys. Lett. **42**, (1976).
[27]J. C. Bellows and P. N. Prasad, J. Chem. Phys. **70**, 1864 (1979).
[28]R. M. Shelby, C. B. Harris, and P. A. Cornelius, J. Chem. Phys. **70**, 34 (1979).
[29]S. F. Fischer and A. Laubereau, Chem. Phys. Lett. **35**, 6 (1975).
[30]J. R. Barrio, G. I. Tolman, N. J. Leonard, R. Spencer, and G. Weber, Proc. Natl. Acad. Sci. (U.S.A.) **70**, 941 (1973).
[31]J. C. Sutherland and M. P. Klein, J. Chem. Phys. **57**, 76 (1972).
[32]A. A. Nevinskii, Opt. Spectrosc. (USSR) **46**, 567 (1979).
[33]P. M. Champion and G. J. Perreault, J. Chem. Phys. (submitted).